

A THEORY FOR NEGATIVE RESISTANCE IN SEMICONDUCTORS

By ROBERT SHERMAN HOPKINS, JR.

An essay submitted to
The Graduate School
of
Rutgers - The State University
for the degree of
Master of Philosophy

Written under the direction of
Professor John A. Sauer
of the Department of Mechanics
and approved by

New Brunswick, New Jersey

May, 1968

ABSTRACT OF THE ESSAY

A Theory for Negative Resistance in Semiconductors

By ROBERT SHERMAN HOPKINS JR., M. Phil.

Essay director: Professor John A. Sauer

A negative resistance has been found in germanium and indium antimonide. The phenomenon can be explained by assuming that a high electric field region exists near the smaller contact on the sample. Carriers are accelerated to their saturation velocity in this high field region. Some of these carriers with a velocity higher than the average velocity have enough energy to jump across the forbidden gap and create a hole-electron pair. This process is called avalanche breakdown. This results in two carrier injection into the bulk of the sample. Materials submitted to high fields and two carrier injection will have a square law current-voltage characteristic. It is shown that if this square law current occurs at a lower voltage than the avalanche breakdown, when avalanche breakdown occurs the newly created holes and electrons will carry the same total current at a lower voltage. Thus there is a negative resistance.

In the case of indium antimonide, whose saturation velocity is quite high, one could have an amplifier, switch, or oscillator operate at a frequency up to 500 GHz for a device thickness of 2 micrometers.

Preface

Acknowledgements

This essay was first written in the spring semester of the 1964-65 school year at Rutgers - The State University as a term paper in Mechanics 411, a course instructed by Prof. J. A. Sauer. The essay was expanded in 1967 to include recent work in the area and then used in partial fulfillment of the requirements for the degree of Master of Science at Rutgers. The essay has again been modified to be used in partial fulfillment of the requirements for the degree of Master of Philosophy at Rutgers to be granted in May 1968.

The author wishes to thank Prof. J. A. Sauer for his interest in the author as a student and for his help in organizing this essay. Thanks are also due to L. F. Eastman with whom the author worked when the original term paper was written and to M. C. Steele for whom the author worked when the original term paper was written. Both were Members of the Technical Staff at RCA Laboratories in Princeton, New Jersey.

Dedication

This essay is dedicated to my wife, Martha Hopkins, whose patience has been appreciated.

Contents

	<u>Page</u>
ABSTRACT	ii
PREFACE	iii
LIST OF ILLUSTRATIONS	v
CHAPTER I <u>INTRODUCTION</u>	1
CHAPTER II <u>THEORY OF THE NEGATIVE RESISTANCE IN</u> <u>GERMANIUM</u>	
Experimental Observations	5
Proposed Model	5
CHAPTER III <u>THE NEGATIVE RESISTANCE IN InSb</u>	16
CHAPTER IV <u>CONCLUSIONS</u>	19
REFERENCES	21
ILLUSTRATIONS	22
VITA	34

List of Illustrations

- Fig. 1-1 Current-voltage characteristics of InSb at 77°K.
From Glicksman and Steele¹.
- Fig. 1-2 Sample as used by Cardona and Ruppel². Oscillations
as observed in the sample.
- Fig. 1-3 Current controlled negative resistance. Voltage
controlled negative resistance.
- Fig. 1-4 Current-voltage characteristics of InSb at 77°K.
From Ando⁴.
- Fig. 1-5 Current-voltage characteristics for p-type InSb slab
with nonsymmetrical ohmic contacts. From Eastman^{5,6}.
- Fig. 2-1 Sketch of sample used in experiments of Steele, Ando,
and Lampert.³ Current-voltage characteristics of sample.
- Fig. 2-2 Sketch of theoretical model.
- Fig. 2-3 Sketch of current as a function of voltage for
region 2 illustrating avalanche breakdown.
- Fig. 2-4 Sketch of current as a function of voltage for region 1
under continuous conditions of double injection.
- Fig. 2-5 Current-voltage characteristics for region 1, region 2,
and entire sample for condition $V_{1A} < V_{1,tr}$. Current-
voltage characteristics when $V_{1A} > V_{1,tr}$. Graphical
explanation of the phenomenon.
- Fig. 2-6 Current-voltage characteristics of proposed model for
the case $V_{1A} > V_{1,tr}$.
- Fig. 3-1 Sketch of sample geometry utilized by Eastman^{5,6}.

CHAPTER I

Introduction

As semiconductor devices become more sophisticated, scientists begin to demand more of them. If one were interested in making a device operate at higher frequencies, he would simply reduce the size of the device to decrease the effect of parasitic elements. If he were interested in making the device handle more power, he would increase the size of the device. Suppose he desired both high frequencies and greater power capabilities. This seemed simple enough. One should try to reduce parasitic elements without reducing the size of the device. However, this will not work if one is too demanding. For a given size, a device has an absolute upper frequency limitation. This occurs because there is a maximum average velocity to which carriers may be accelerated.

In general, the conduction of current is given by a matrix-vector product

$$\underline{J} = \underline{\sigma} \cdot \underline{E} \quad (1-1)$$

where \underline{J} is a vector representing current density, \underline{E} is a vector representing the electric field, and $\underline{\sigma}$ is a matrix representing the conductivity of the media.

In a linear, isotropic, homogeneous media, the matrix $\underline{\sigma}$ reduces to a scalar σ . In this case one also finds the relationship between current density and velocity to be

$$\underline{J} = n e \langle \underline{v} \rangle \quad (1-2)$$

where n is the carrier concentration, e the electronic charge, and $\langle \underline{v} \rangle$ the average velocity of the carriers. Then for this media

$$\langle \mathbf{v} \rangle = \frac{1}{n e} \underline{J} \quad (1-3)$$

$$= \frac{\sigma}{n e} \underline{E} \quad (1-4)$$

To sweep a charge through a device of length L and back again would require a time

$$T = \frac{2 L}{v} \quad (1-5)$$

or

$$T = \frac{2 L n e}{\sigma E} \quad (1-6)$$

where E is the magnitude of the electric field in the direction of L . Thus one can, according to equation (1-6), reduce this time to any arbitrary value by applying a large enough electric field. This is not true. Neither equation (1-1) nor (1-4) holds for large fields. The velocity increases with electric field only till the maximum velocity is reached. Let this velocity be designated v_{sat} . Then the minimum time involved to sweep a charge through the device and back again will be

$$T_{\text{min}} = \frac{2 L}{v_{\text{sat}}} \quad (1-7)$$

Thus the maximum frequency at which such a device will be useful is

$$f_{\text{max}} = \frac{1}{T_{\text{min}}} \quad (1-8)$$

$$= \frac{v_{\text{sat}}}{2 L} \quad (1-9)$$

Obviously one is interested in examining this carrier velocity saturation because the maximum frequency of a device is proportional to the saturation velocity. Also, one would like to understand the phenomenon. In 1958 while investigating carrier velocity saturation

in Indium Antimonide (InSb), Glicksman and Steele¹ reported that very small increases in the applied electric field above some critical value caused very large increases in the current density as shown in Fig. (1-1). They attributed it to impact ionization across the forbidden gap with the resultant creation of electron-hole pairs. This was the first detailed report of such an effect in bulk semiconductor with no junctions.

Then in 1960 while making high electric field measurements, Cardona and Ruppel² observed current oscillations in p-type germanium (Ge) crystals of 23, 14, and 4.2 ohm cm. No oscillations were observed in n-type. A tin soldered contact was made at one end and a metal point contact was placed on the opposite end of each sample. See Fig. (1-2) for a diagram of the crystal and an example of their observation. The point contact had to be rectifying. The point contact was forward biased and a 50 ohm resistor was placed in series with the sample. The voltage was pulsed to avoid overheating the crystal. With a current of about 10 mA there were oscillations in the current at a frequency of 5 KHz to 5 MHz. They reported that no negative resistance was observed.

In 1962 Steele, Ando, and Lampert³ reported on new experiments with Ge and proposed an explanation. They observed current controlled negative resistances with all diodes (both p-type and n-type) which exhibited oscillations. Current controlled negative resistance means that the voltage as a function of the current is a single valued function and that there is a portion of the curve whose slope is negative. Voltage controlled negative resistance means that the current as a function of the voltage is a single valued function

and that there is a portion of the curve whose slope is negative, as for a tunnel diode. See Fig. (1-3) for an example. They felt that the oscillations were relaxation oscillations dependent upon the existence of the negative resistance. Avalanche breakdown at the point contact resulted in two carrier current flow. The reduction of voltage at constant current (the negative resistance) is a consequence of the fact that the current in the semiconductor after breakdown is a two carrier current which is carried at a lower voltage than if it were a pure ohmic current.

In 1964 Ando⁴ observed oscillations and a large current controlled negative resistance in p-type InSb at 77°K. He explained that this was the same effect as was observed in Ge by Steele, Lampert, and himself. Fig. (1-4) is a copy of the I-V characteristic he reported.

In 1965 Eastman^{5,6} reported a new negative resistance effect in InSb. Nonsymmetrical contacts were formed on the InSb. The negative resistance occurred when the small contact was made positive. It was different from that reported by Ando for three reasons: 1) The polarity was reversed; 2) The current did not rise linearly with voltage before breakdown; and 3) The negative resistance magnitude was much lower. Also, both Eastman and Ando reported vertical regions of the curve rather than square law as observed in Ge. As a result a slightly different model had to be formed. Again, avalanche breakdown was the essential factor involved in the negative resistance. See Fig. (1-5) for a comparison.

The purpose, then, of this essay is to present the results of these various scientists in one paper and account for all effects observed.

CHAPTER II

Theory of the Negative Resistance in Germanium

Experimental Observations

The experiments of Steele, Ando, and Lampert³ were conducted with many Ge single crystals. Both p-type and n-type crystals were studied. The resistivities ranged from .1 ohm cm. to 50 ohm cm. The crystals had a point contact on one end and an ohmic contact on the other. These diodes were forward biased. It was felt that the presence of minority carriers in the body of the diode was essential to the effect because the negative resistance was not seen with reverse bias. These minority carriers would be present after avalanche breakdown if the diode were forward biased. Oscillations were observed from about 1 KHz to 10 MHz.

A variety of diode body shapes were used, but a bridge structure shown in Fig. (2-1a) was reported. The fact that a negative resistance was observed at internal points a-b shows clearly that the entire body participated in the negative resistance. The I-V characteristics are shown in Fig. (2-1b). Curve e-e' is the I-V characteristic for the entire structure. Curve a-b was measured simultaneously. This clearly attests to the fact that the bulk of the semiconductor plays an important role in the phenomenon.

Proposed Model

Assume that one has a single crystal of Ge, p-type material, with the geometric structure given in Fig. (2-2). Each part is a cylinder of diameter D_1 or D_2 and length of L_1 or L_2 . Apply a potential difference of V volts to the crystal and determine the

potential drop across regions 1 and 2.

$$R_1 = \frac{L_1 \rho}{\frac{\pi D_1^2}{4}} \quad (2-1a)$$

$$R_2 = \frac{L_2 \rho}{\frac{\pi D_2^2}{4}} \quad (2-1b)$$

where ρ is the resistivity of the material and assumed perfectly homogeneous.

$$V_1 = \frac{V R_1}{R_1 + R_2} \quad (2-2)$$

$$= \frac{4 V L_1 \rho}{\pi D_1^2} \left[\frac{4 \rho L_1}{\pi D_1^2} + \frac{4 \rho L_2}{\pi D_2^2} \right]^{-1} \quad (2-3)$$

$$= \frac{\frac{V L_1}{D_1^2}}{\frac{L_1}{D_1^2} + \frac{L_2}{D_2^2}} \quad (2-4)$$

$$= \frac{V}{1 + \frac{L_2 D_1^2}{L_1 D_2^2}} \quad (2-5a)$$

$$V_2 = \frac{V}{1 + \frac{L_1 D_2^2}{L_2 D_1^2}} \quad (2-5b)$$

Now determine E_1 and E_2 , the electric fields in regions 1 and 2.

$$E_1 = \frac{V_1}{L_1} \quad (2-6a)$$

$$E_2 = \frac{V_2}{L_2} \quad (2-6b)$$

Because of continuity of current one must have

$$I_1 = I_2 \quad (2-7)$$

As a result

$$\frac{V_1}{R_1} = \frac{V_2}{R_2} \quad (2-8)$$

Then

$$\frac{V_1}{V_2} = \frac{R_1}{R_2} \quad (2-9)$$

From (2-6a) and (2-6b) one obtains

$$\frac{V_1}{V_2} = \frac{L_1 E_1}{L_2 E_2} \quad (2-10)$$

Substituting (2-10) into (2-9)

$$\frac{R_1}{R_2} = \frac{L_1 E_1}{L_2 E_2} \quad (2-11)$$

Then

$$\frac{E_1}{E_2} = \frac{L_2 R_1}{L_1 R_2} \quad (2-12)$$

$$= \frac{L_2 \rho \frac{4L_1}{\pi D_1^2}}{L_1 \rho \frac{4L_2}{\pi D_2^2}} \quad (2-13)$$

And finally

$$\frac{E_1}{E_2} = \frac{D_2^2}{D_1^2} \quad (2-14)$$

If we specify

$$D_1^2 \gg D_2^2 \quad (2-15)$$

then we obtain

$$E_2 \gg E_1 \quad (2-16)$$

Let us assume a one carrier system for the moment and determine the current density which results in region 2. Assume the carriers are holes.

$$J_2 = \sigma E_2 \quad (2-17)$$

$$= \sigma \frac{V_2}{L_2} \quad (2-18)$$

But

$$\sigma = p \mu_p e \quad (2-19)$$

Thus

$$J_2 = p \mu_p e \frac{V_2}{L_2} \quad (2-20)$$

where p is the number of holes present and μ_p the mobility of the holes.

Now let us begin to increase V . As V increases, V_2 increases and also E_2 increases. From the results of Glicksman and Steele¹ which were discussed in Chapter I, we know that there is a critical field E_{2A} which when reached will cause impact ionization to occur in region 2. Recalling that $E_2 \gg E_1$, equation (2-16), we realize that this breakdown has occurred in region 2 but not in region 1. Let I_A be the current flowing when impact ionization occurred. It should be pointed out here that our power source must be a current source since the negative resistance is current controlled. When

we speak of increasing V , we really increase I and then V will increase.

Now

$$V_{2A} = E_{2A} L_2 \quad (2-21)$$

From equation (2-10)

$$V_{1A} = \frac{L_1}{L_2} \frac{E_{1A}}{E_{2A}} V_{2A} \quad (2-22)$$

and from equation (2-14)

$$= \frac{L_1}{L_2} \frac{D_2^2}{D_1^2} V_{2A} \quad (2-23)$$

Thus the voltage across the entire crystal when breakdown occurs in region 2 is given by

$$V_A = V_{1A} + V_{2A} \quad (2-24)$$

$$= V_{2A} \left(1 + \frac{L_1}{L_2} \frac{D_2^2}{D_1^2} \right) \quad (2-25)$$

The linear portion of the graph of Fig. (2-3) shows ohmic characteristics for low voltages while the vertical portion shows the current increasing without limit at a constant voltage in region 2 after breakdown has occurred in that region. Notice that this curve is an idealized copy of Fig. (1-1), the actual data of Glicksman and Steele¹.

After this breakdown occurs, many electrons and just as many new holes are created in region 2. These newly generated carriers will be available for injection into region 1. Recall that we are discussing p-type material. Thus there are already many holes in region 1. If we now bias the device so that region 1 is positive with respect to region 2, the newly generated electrons can be

injected into region 1. Since holes were already present in region 1 and since we are now injecting electrons into region 1, we have a two-carrier system in region 1. This is known as double injection.

Now it becomes necessary for us to discuss double injection to further understand what is happening. Double injection is the simultaneous injection of electrons from a negative contact and holes from a positive contact. This problem has already been solved by Lampert and Rose⁷. The current voltage characteristic will be given by

$$J_1 = P_0 \mu_p e \frac{V_1}{L_1} \quad V_1 < V_{1,tr} \quad (2-26)$$

and

$$J_1 = P_0 \mu_p \mu_n e \tau \frac{V_1^2}{L_1^3} \quad V_1 > V_{1,tr} \quad (2-27)$$

where P_0 is the original hole density in the material before double injection began, μ_n the electron mobility, μ_p the hole mobility, τ the effective lifetime for the injected electrons and holes, and $V_{1,tr}$ the transition voltage at which the transition from ohmic conduction to square law conduction occurs. For low fields one has ohmic conduction, and for high fields, one has square law conduction. For instance, if a low field is applied, the injected electrons and holes will be moving at a low velocity since

$$v_n = \mu_n E \quad (2-28a)$$

$$v_p = \mu_p E \quad (2-28b)$$

Thus, because of the low velocity of the carriers, the electrons

and holes are certain to recombine. This would then leave the original P_0 holes to carry the entire current and one has ohmic conduction. One would certainly expect equation (2-26) to be correct for low fields. Suppose, however, a higher field were applied. One could expect the injected electrons and holes, which now have a higher velocity, to be carried entirely through L_1 so fast that they do not have time to recombine. It is not intuitively obvious that one should then have square law conduction, but it should be obvious that the conduction is not ohmic. The critical potential at which this transition occurs is given by a simultaneous solution of equations (2-26) and (2-27). This voltage is

$$V_{1,tr} = \frac{L_1^2}{\mu_n \tau} \quad (2-29)$$

The I-V characteristics for region 1 under conditions of double injection are given in Fig. (2-4).

For the arguments that follow it is necessary for one to assume a constant current circuit. Everything previously discussed certainly will continue to be true. Now we have I as the independent variable.

Recalling that V_{1A} was the voltage across region 1 when impact ionization occurred in region 2, we must find what relationships, if any, exist between V_{1A} and $V_{1,tr}$. Copying equation (2-23)

$$V_{1A} = \frac{L_1 D_2^2}{L_2 D_1^2} V_{2A} \quad (2-23)$$

Substituting from (2-21)

$$V_{1A} = \frac{D_2^2}{D_1^2} E_{2A} L_1 \quad (2-30)$$

Then from equations (2-29) and (2-30)

$$\frac{V_{1A}}{V_{1,tr}} = E_{2A} \frac{D_2^2 \mu_n \gamma}{D_1^2 L_1} \quad (2-31)$$

There are no variables on the right hand side of (2-31). E_{2A} is a critical field at which impact ionization will occur in this particular crystal. D_2 and D_1 are most certainly constant, as is L_1 . The mobility μ_n is constant in this case because it is the minority carrier in the low field region. Recall that this mobility entered the equations because minority carriers were injected into region 1 when impact ionization occurred in region 2. The recombination lifetime γ should also be constant. Thus there is a relationship of some sort between these two critical values of voltage. Let us consider two situations:

$$\text{Case 1} \quad V_{1A} < V_{1,tr} \quad (2-32)$$

$$\text{Case 2} \quad V_{1A} > V_{1,tr} \quad (2-33)$$

Case 1 --- In this case, impact ionization occurs at a lower voltage than does square law double injection current. As a result when impact ionization occurs in region 2, there will be only ohmic current in region 1. At a somewhat higher voltage, square law conduction will begin. Nothing significant has really occurred.

Case 2 --- Now square law double injection current can be sustained at a lower voltage than impact ionization occurs. Thus, soon as impact ionization occurs in region 2, we will have square law conduction current in region 1. The voltage across region 1 the instant before impact ionization is V_{1A} . The voltage across region 2 the instant before impact ionization is V_{2A} . The voltage

across region 2 the instant after impact ionization will be V_{2A} . For verification of this, see Fig. (2-3). For constant current, the voltage across region 1 the instant after impact ionization is constrained to be on the square law conduction curve since double injection is now taking place. Before this instant the voltage was constrained to the ohmic portion of the curve since there was no double injection prior to impact ionization. Notice however, that in moving from ohmic conduction to square law conduction, the voltage across region 1 has decreased. Since the voltage across region 2 remained constant, the voltage across the entire device has decreased. Fig. (2-5) illustrates Case 1 and Case 2 quite vividly. Fig. (2-6) shows the theoretical I-V characteristics of the entire device. Notice how favorably it compares to Fig. (2-1b).

One important point to note is that the negative resistance is a consequence of double injection resulting from impact ionization, or avalanche breakdown. Neither the double injection nor the avalanche breakdown occurring separately could cause the phenomenon to occur, but rather the combination and in the proper order.

One may raise a question because the experimental curve indicates a non-zero slope for the negative resistance portion of the curve and the theoretical curve indicates a zero slope for this portion. Two points may be made here: 1) The experimental curve was plotted using a ramp of current; when a point by point measurement was made, the slope appeared to be zero. 2) In the theoretical model, we have assumed impact ionization to occur in the entire region 2 at the same instant; actually this would not be true in practice. The reason the point by point measurement

indicated a zero slope was that the current source was not stiff enough. A zero slope infers an infinite negative resistance. The impedance of the current source must be greater in magnitude than the impedance of the negative resistance or there will be no stable bias point in the negative resistance region.

The requirement for seeing a negative resistance is given by equation (2-33)

$$V_{1A} > V_{1,tr} \quad (2-33)$$

Interpreting this in equation (2-31) leads to the following set of criterion: a) To see a negative resistance in p-type material one must satisfy the requirement:

$$E_{2A} \frac{D_2^2 \mu_n \tau}{D_1^2 L_1} > 1 \quad (2-34)$$

b) To see a negative resistance in n-type material one must satisfy the requirement:

$$E_{2A} \frac{D_2^2 \mu_p \tau}{D_1^2 L_1} > 1 \quad (2-35)$$

Since $\mu_n > \mu_p$ for Ge, it becomes obvious that the negative resistance is more easily obtained in p-type material than in n-type material. You will recall that Cardona and Ruppel² observed oscillations in p-type material only.

There is one bad assumption which was made for the theoretical model which will be discussed briefly. We assumed the carrier velocity to be given by equations (2-28)

$$v = \mu E \quad (2-36)$$

However, for larger fields this relation does not hold as was

discussed in Chapter I. It was pointed out that the carriers reach a maximum average velocity denoted by v_{sat} . Experimental investigations show that the velocity v_{sat} is not high enough to produce impact ionization. However, v_{sat} is only the average velocity. There will be a few carriers in the tail of the distribution with the necessary velocity. These are normally called hot carriers⁸. One can determine the velocity necessary for impact ionization from the relation

$$E_v = \frac{1}{2} m_o v^2 \quad (2-37)$$

where m_o is the effective mass and E_v the bandgap of the material.

CHAPTER IIIThe Negative Resistance in InSb

In 1964 Ando⁴ announced that he had obtained a negative resistance in p-type InSb at 77°K. The polarity of the electric field was the same as in the Ge experiments of Chapter II. He used calculations given by Steele, Ando, and Lampert³ and found great agreement between the theory and experimental results. Ando was working with InSb because the mobility of the electrons in InSb is greater than the mobility of the electrons in Ge. This means that the injected minority carriers of region 1 will have a greater velocity and will move through that region in less time. Thus an even lower voltage will sustain the same current and a greater dynamic range of the negative resistance will be observed. This was, in fact, observed. Also, the saturation velocity in InSb is greater than that of Ge. This means that the minimum time required to sweep a carrier through a given piece of the material and back again is reduced. Thus the maximum frequency is increased. Ando reported oscillations of 31 MHz. The maximum frequency reported for Ge for the same dimensions was 10 MHz. The data Ando reported is given in Fig. (1-4).

Then in 1965, Eastman⁵ announced that he had obtained a new negative resistance in InSb. The samples were made much thinner to get a faster transit time. He did not use a point contact, rather he had two nonsymmetrical ohmic contacts, as in Fig. (3-1). There were differences in the results obtained by Eastman and Ando. These were:

- 1) The polarity was reversed

2) The current did not rise linearly with voltage before breakdown

3) The magnitude of the negative resistance was much lower.

There was also one great difference between the Ge results and these results with InSb: After the negative resistance, the curve becomes nearly vertical rather than rising with a voltage squared dependence. The I-V characteristics of the device are shown in Fig. (1-5)

The revised theory proposes that the current density has a fixed geometry in the low current linear region of the characteristic curve. The maximum current density is located at the center of the small contact and begins to saturate at higher currents. Thus the current will tend to fringe out around this saturated region. This will continue until the entire contact has a saturated current density. Because of the fringing, a small increase in current will cause a greater increase in the voltage. Thus the sublinear portion of the curve is accounted for. As the current continues to rise, the electric field near the small contact becomes high enough to cause impact ionization to occur near the small contact. In this case hot electrons⁸ cause the impact ionization rather than the holes, the majority carrier. This accounts for the polarity reversal. Further increase of the current causes the impact ionization region to extend throughout the entire device. Since this is a gradual occurrence, one obtains a controllable negative resistance. Finally, there is an impact ionization region extending completely from the small electrode to the large electrode. Thus one finds that the curve should indeed be vertical for high current levels.

Notice that we have not altered the theory originally proposed by Steele, Ando, and Lampert. All the experimental discrepancies are a result of a different geometry and a different material.

CHAPTER IVConclusions

A negative resistance device can be very handy. For instance, assume a transmission line is terminated with a negative resistance. The reflection coefficient is

$$\rho = \frac{Z_L - Z_0}{Z_L + Z_0} \quad (4-1)$$

The load is

$$Z_L = -R \quad (4-2)$$

Then

$$\rho = \frac{-R - Z_0}{-R + Z_0} \quad (4-3)$$

$$= - \frac{1 + \frac{R}{Z_0}}{1 - \frac{R}{Z_0}} \quad (4-4)$$

Thus

$$\rho > 1 \quad (4-5)$$

This means more is reflected than is incident. Or in other words, we have an amplifier.

A negative resistance is very good as a switch. The InSb negative resistance should perform this function quite well because the two stable states are separated well enough to have good definition.

Another very important capability of a negative resistance device is to function as an oscillator. In fact, it was this property which first exposed the phenomenon.

Because of the high saturation velocity of electrons in InSb, it will perform all the functions listed above quite well at high frequencies. Amplifiers, switches, and oscillators which operate in very short times are always in demand. Since this effect is a transit time effect, making a smaller device will speed it up. Equation (1-9) tells us how high in frequency this device will work:

$$f_{\max} = \frac{v_{\text{sat}}}{2L} \quad (1-9)$$

Using the saturation velocity of $1 \cdot 10^8$ cm./sec. and a thickness of 2 micrometers, one finds that this device will work up to 500 GHz.

This device has one tremendous problem. It must be cooled to 77°K. Eastman made some preliminary temperature measurements and found that the negative resistance disappeared around 210°K. Usually one prefers to not have to cool devices this much to get them to operate.

There are several questions that should be answered in future work:

- 1) Can the InSb device operate at higher temperatures in the presence of a magnetic field?
- 2) Is there some other material as fast as InSb which does not need to be cooled to exhibit this phenomenon?
- 3) Are there any other effects which begin to appear as one makes the device smaller than the 25 micrometers of Eastman?

References

- 1 M. Glicksman and M. C. Steele, Physical Review, Vol. 110, No. 5, pp. 1204-1205, June 1958.
- 2 M. Cardona and W. Ruppel, Journal of Applied Physics, Vol. 31, pp. 1826-1827, 1960.
- 3 M. C. Steele, K. Ando, and M. A. Lampert, Journal of the Physical Society of Japan, Vol. 17, No. 11, pp. 1729-1736, Nov. 1962.
- 4 K. Ando, Japanese Journal of Applied Physics, Vol. 3, No. 12, pp. 757-760, Dec. 1964.
- 5 L. F. Eastman, Proc. of the IEEE, pp. 761-762, July 1965.
- 6 L. F. Eastman, IEEE Trans. on Electron Devices, Vol. ED-13, No. 1, pp. 117-121, Jan. 1966.
- 7 M. A. Lampert and A. Rose, Physical Review, Vol. 121, No. 1, pp. 26-37, Jan. 1961.
- 8 M. Glicksman and W. A. Hicinbothem, Jr., Physical Review, Vol. 129, No. 4, pp. 1572-1577, Feb. 1963.

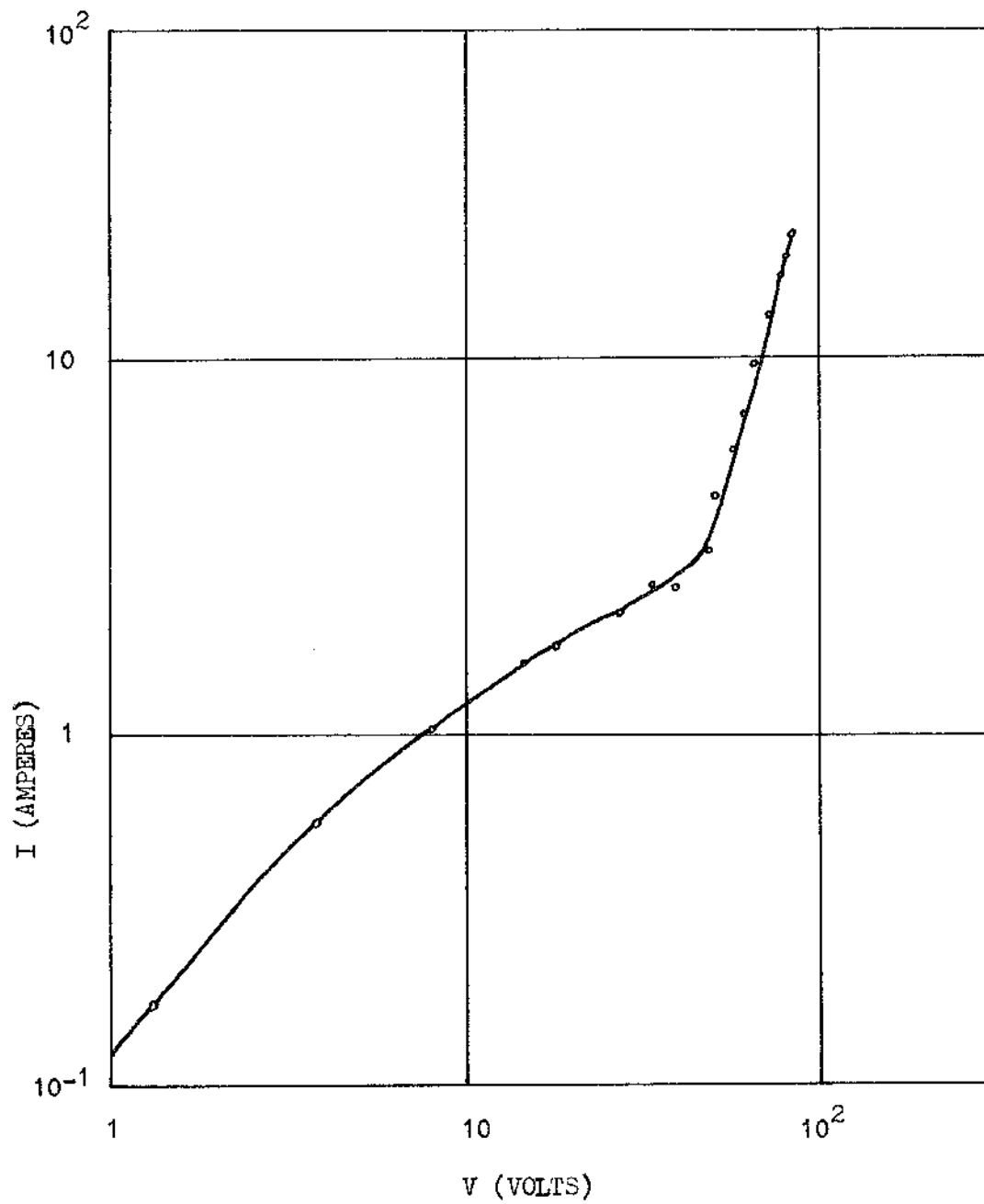
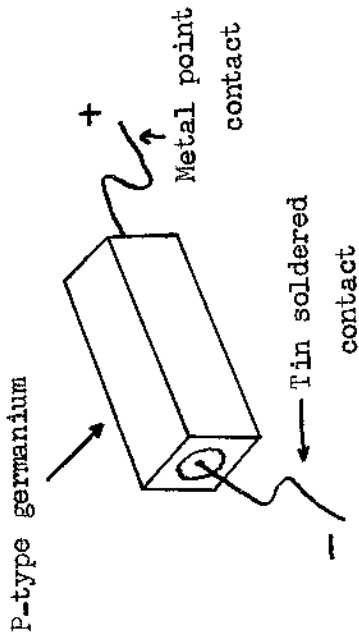
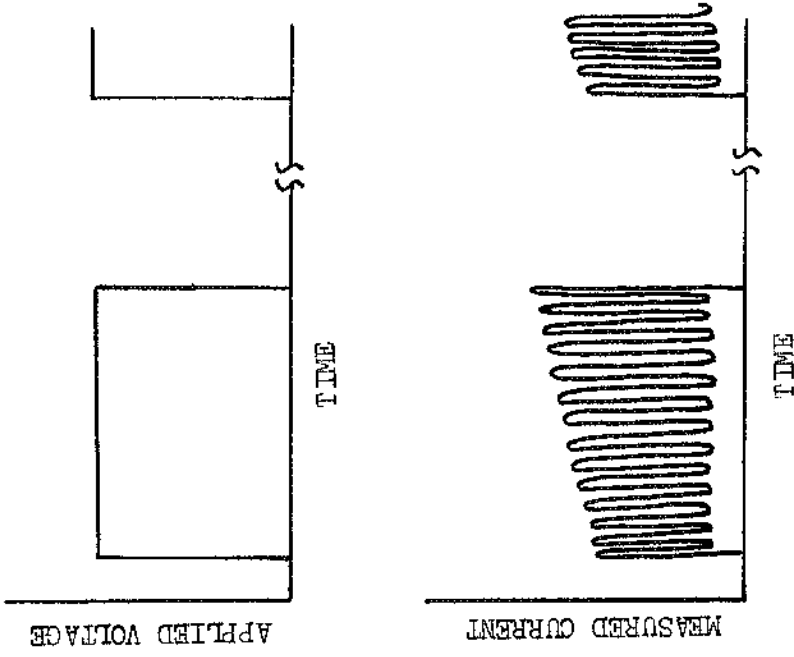


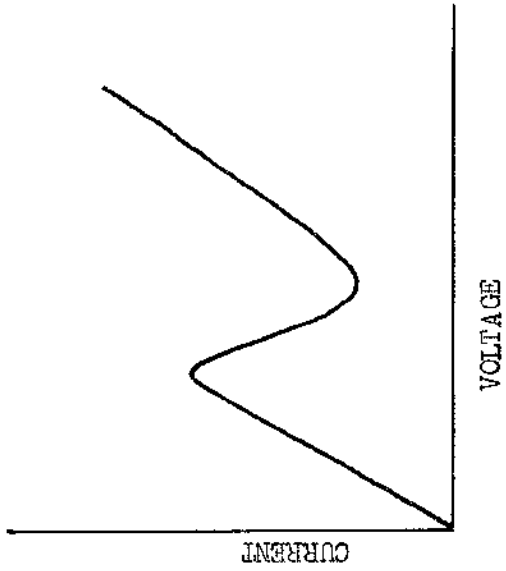
Fig. 1-1 Current-voltage characteristic of InSb at 77°K .
From Glicksman and Steele¹.



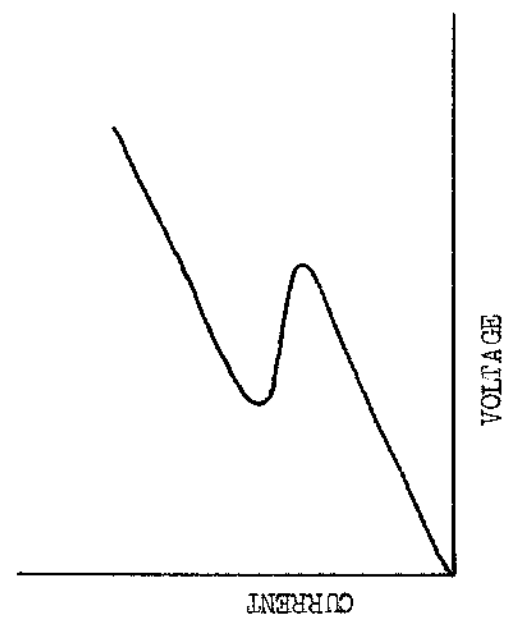
b.

a.

Fig. 1-2 a. Sample as used by Cardona and Ruppel.²
b. Oscillations as observed in sample of a.



a.



b.

Fig. 1-3 a. Current controlled negative resistance.
 b. Voltage controlled negative resistance.

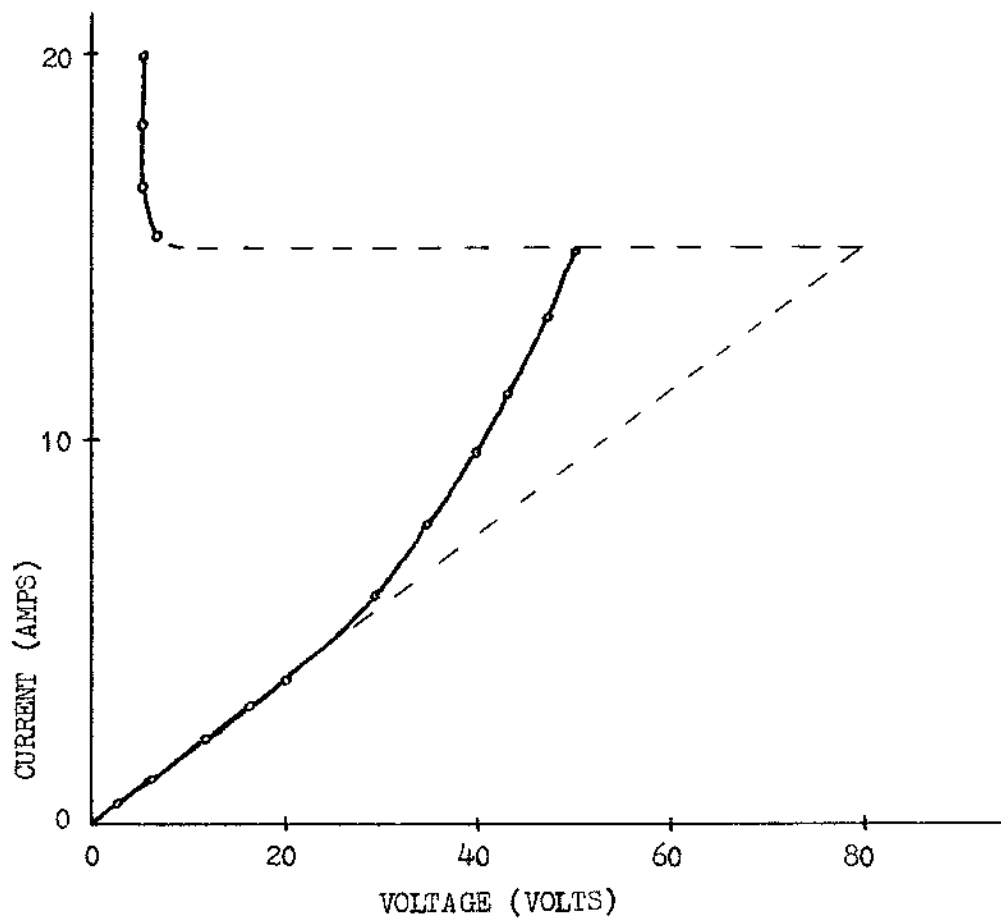


Fig. 1-4 Current-voltage characteristics of InSb at 77°K. From Ando⁴.

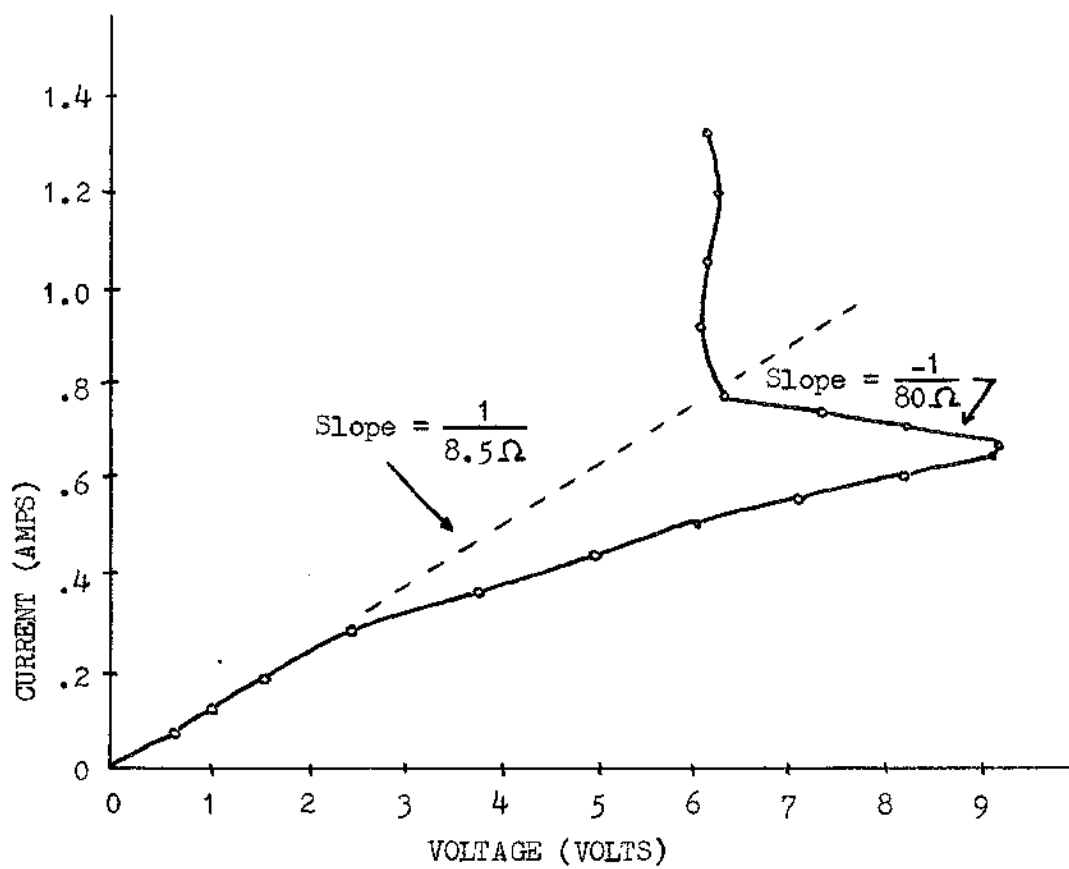
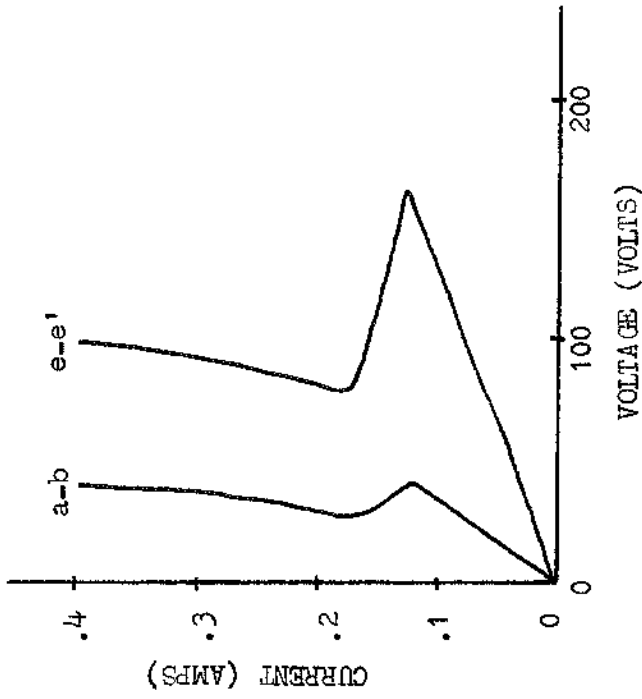
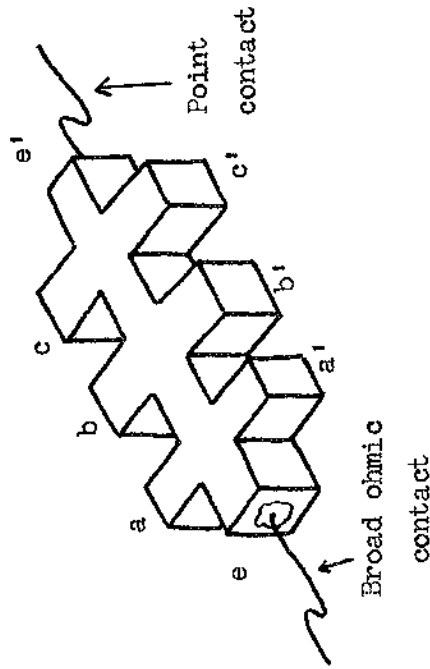


Fig. 1-5 Current-voltage characteristics for P-type InSb slab with nonsymmetrical ohmic contacts. From Eastman^{5,6}.



b.



a.

Fig. 2-1 a. Sketch of sample used in experiments of Steele, Ando, and Lampert³.
 b. Current-voltage characteristics of sample above. Curves were obtained simultaneously.

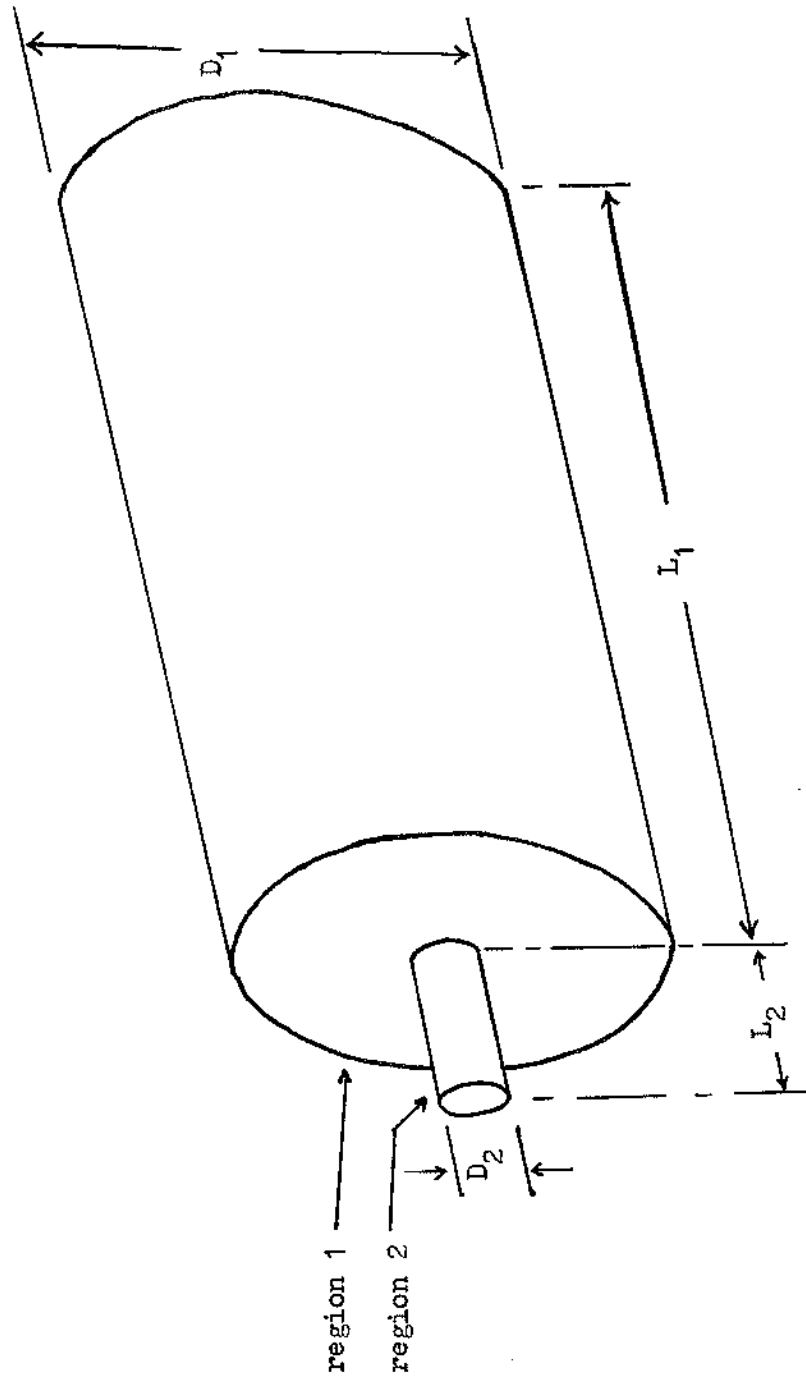


Fig. 2-2 Sketch of theoretical model.

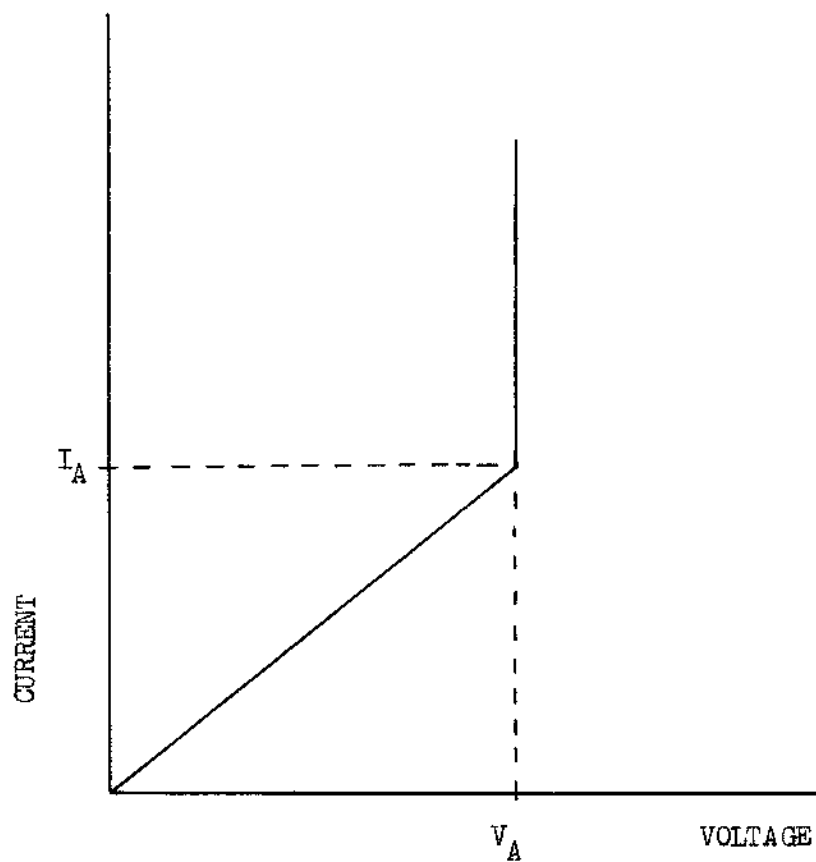


Fig. 2-3 Sketch of current as a function of voltage for region 2 illustrating avalanche breakdown.

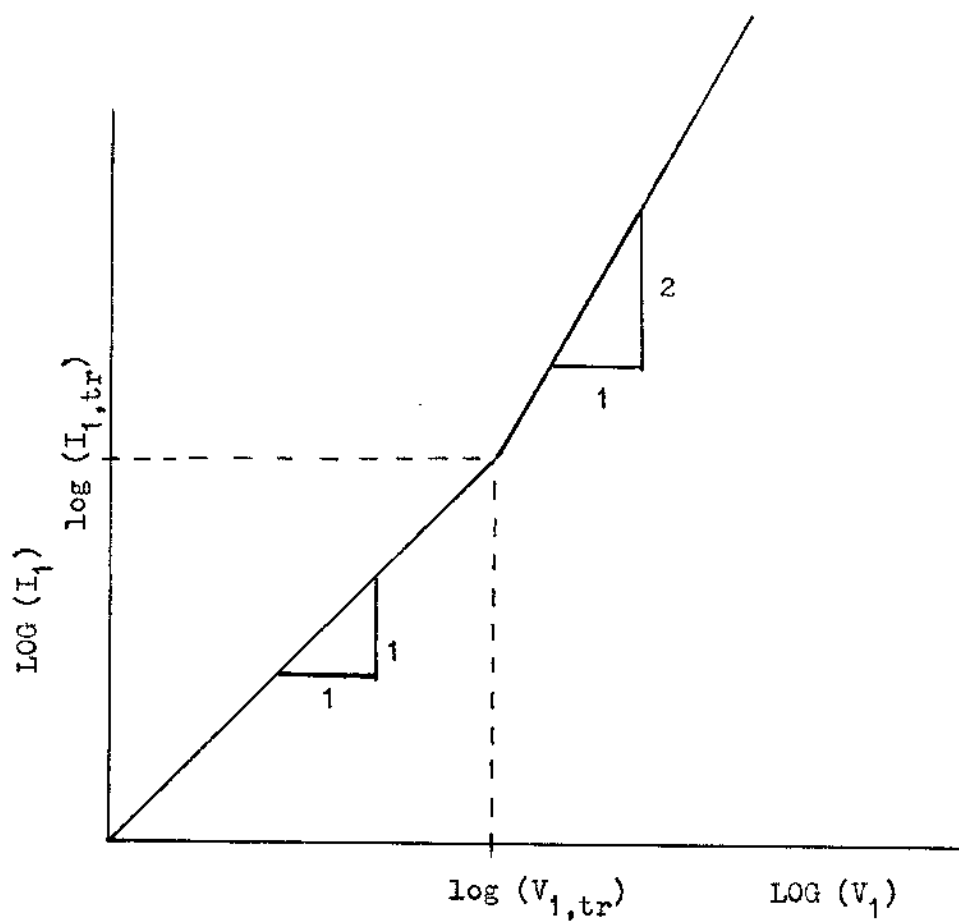


Fig. 2-4 Sketch of current as a function of voltage for region 1 under continuous conditions of double injection. Square law conduction cannot be supported for low voltages (low fields).

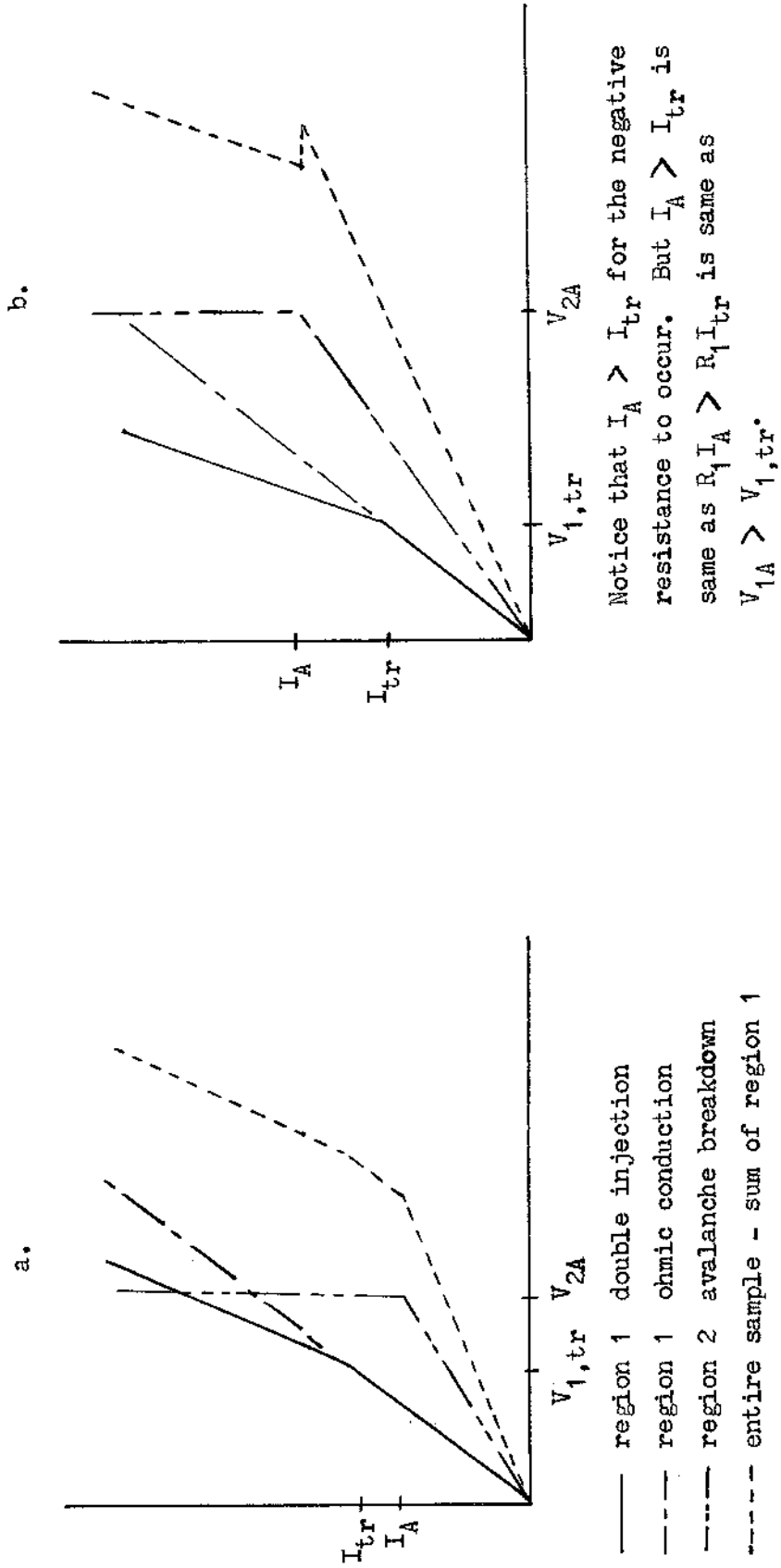


Fig. 2-5 a. I - V characteristics for region 1, region 2, and entire sample for condition $V_{1A} < V_{1,tr}$.

b. I - V characteristics when $V_{1A} > V_{1,tr}$.

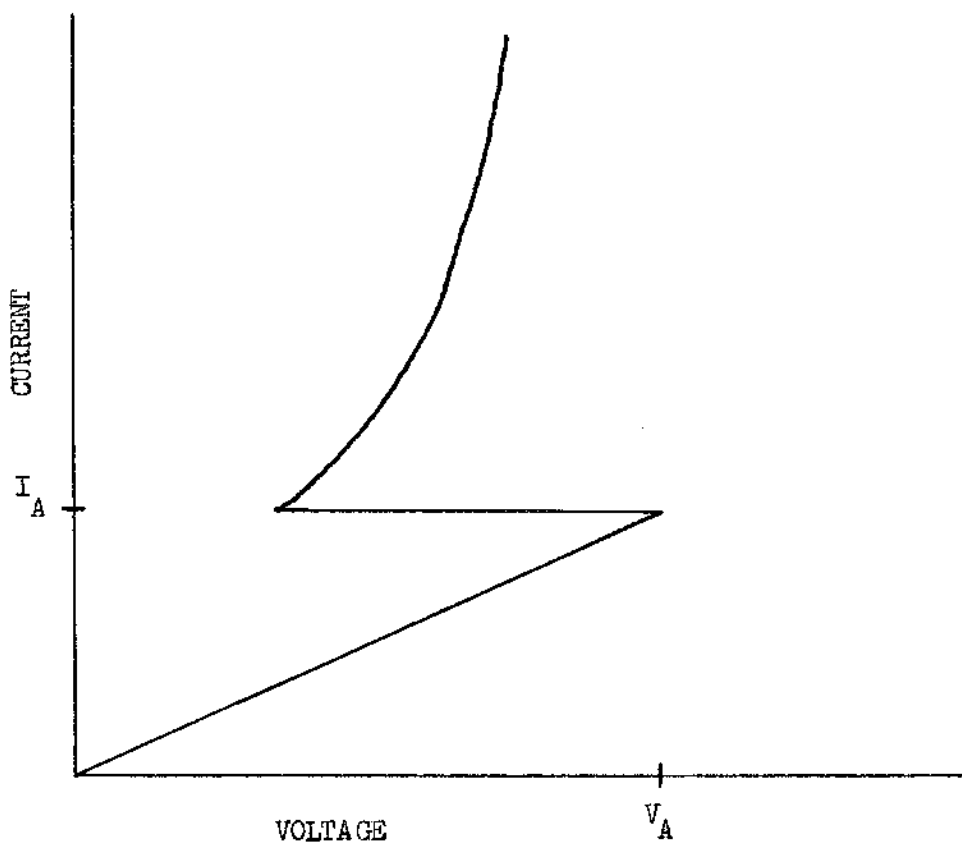


Fig. 2-6 I - V characteristics of proposed model for the case $V_{1A} > V_{1,tr}$.

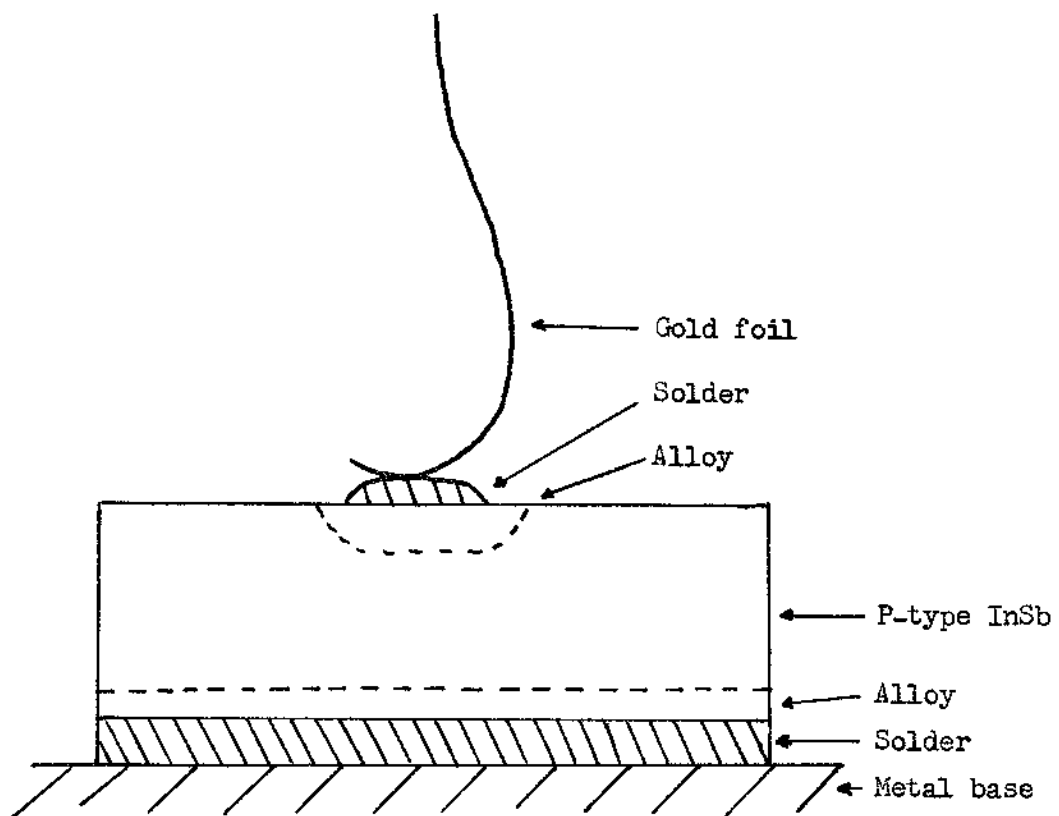


Fig. 3-1 Sketch of sample geometry utilized by Eastman^{5,6}.

Robert Sherman Hopkins Jr.

- 1942 Born October 26 in Bevinsville, Kentucky
- 1960 Graduated from Holton High School, Holton, Indiana
- 1963-64 Junior Engineer, Arvin Electronics Laboratory
West Lafayette, Indiana
- 1964 B.S.E.E., Purdue University
- 1964- Member of the Technical Staff, RCA Laboratories
Princeton, New Jersey
- 1964-66 RCA Laboratories Graduate Study Program
- 1966-67 RCA Laboratories Doctoral Study Award
- 1967 M.Sc. in E.E., Rutgers - The State University
- 1968 M.Phil. in E.E., Rutgers - The State University